Solid-state slit camera (SSC) onboard MAXI

Hiroshi Tomida,[1] Masaru Matsuoka,[1] Kazuyoshi Kawasaki,[1] Shiro Ueno,[1]
Yasuki Adachi,[1] Mitsuhiro Kohama,[1,2] Motoko Suzuki,[1] Masaki Ishikawa,[1,9]
Haruyoshi Katayama,[1] Tatehiro Mihara,[2] Mutsumi Sugizaki,[2] Naoki Isobe,[2]
Hiroshi Tsunemi,[3] Emi Miyata,[3] Nobuyuki Kawai,[4] Jun Kataoka,[4]
Atsumasa Yoshida,[5] Kazutaka Yamaoka,[5] Hitoshi Negoro,[6] Motoki Nakajima,[6]
Yoshihiro Ueda,[7] Mikio Morii,[8] and MAXI team

[1] Japan Aerospace Exploration Agency (JAXA), Sengen 2-1-1, Tsukuba, Ibaraki, Japan
[2] The Institute of Physical and Chemical Research (RIKEN), Hirosawa 2-1, Wako, Saitama, Japan
[3] Osaka Unversity, Machikaneyama 1-1, Toyonaka, Osaka, Japan
[4] Tokyo Institute of Technology, Ookayama 2-12-1, Meguro, Tokyo, Japan
[5] Aoyama Gakuin University, Fuchinobe 5-10-15, Sagamihara, Kanagawa, Japan
[6] Nihon University, Kanda Surugadai 1-8-14, Chiyoda, Tokyo, Japan
[7] Kyoto University, Kita-Shirakawa Oiwakecho, Sakyo, Kyoto, Kyoto, Japan
[8] Rikkyo University, Nishi-Ikebukuro 3-34-1, Toshima, Tokyo, Japan
[9] Graduate Unversity for Advanced Study (Sokendai), Shonan Village, Hayama, Kanagawa, Japan
E-mail(HT): tomida.hiroshi@jaxa.jp

Abstract

SSC (Solid-state Slit Camera) is an X-ray camera onboard the MAXI mission. SSC consists of two SSC unit (SSCU) and SSC electronics (SSCE). SSCU includes 32 X-ray CCDs, slit and slat system, and so on. SSCE controls SSCU. SSC covers 0.5 – 12keV with energy resolution of <150eV at 5.9keV. CCDs are operated at –60°C utilizing thermo-electric cooler, loop heat pipe, and passive radiators.

Key words: All-Sky-Monitor, X-ray detector, CCD, soft X-ray

1. Introduction

CCD (charge-coupled device) has been nominal X-ray detector as photon counting device since the successful operation of SIS onboard the ASCA satellite (Burke *et al.* 1991). Its good position resolution and moderate energy resolution are suitable for X-ray astronomical observations. SSC (Solid-state Slit Camera), which is an X-ray camera of MAXI mission, also employs X-ray CCDs for X-ray detections. SSC has many characteristics different from GSC, another X-ray camera of MAXI (Mihara *et al.* (this proceedings)). The main objectives of SSC would be all-sky monitor in lower energy band, and the spectroscopy of largely extended celestial objects such as galactic ridge emission, Vela SNR, and so on. This paper describes the basic design and performances of the SSC system.

2. SSC System

The SSC system is composed of two SSC Units (SSCUs) and SSC Electronics (SSCE). Figure 1 shows the block diagram of SSC.

SSCU is a sensor part of SSC. One SSCU includes X-ray CCDs, preamplifiers, multiplexers, slit-collimator system, calibration sources, and so on. Figure 2 shows the schematic view and photograph of SSCUs. One of SSCUs monitors X-ray sky in the horizontal direction of MAXI, and another is for zenith direction. Hence, the former is called SSCU-H, and another is called SSCU-Z.

SSCE controls SSCUs. SSCE generates CCD drive signal according to commands from DP (data processor), and digitizes the video signal from SSCU. The Digitized data are transferred to DP. SSCE also controls CCD temperature using thermo-electric cooler (TEC) embedded in CCD chips.

Radiator and heat pipe are not a portion of SSC, however, they are very important to cool X-ray CCDs (section 5.). DP is also not a portion of SSC, although the data reduction in DP is essential to maximize the data quality of X-ray events (section 3.).

2.1. X-ray CCD

A photograph of an MAXI-CCD is shown in Figure 3. CCDs are FFTCCD-4673 fabricated by Hamamatsu Photonics K.K.[1] . The chip is front-illuminated and two-phase CCD operated in full frame transfer mode.

*1 http://www.hamamatsu.com/

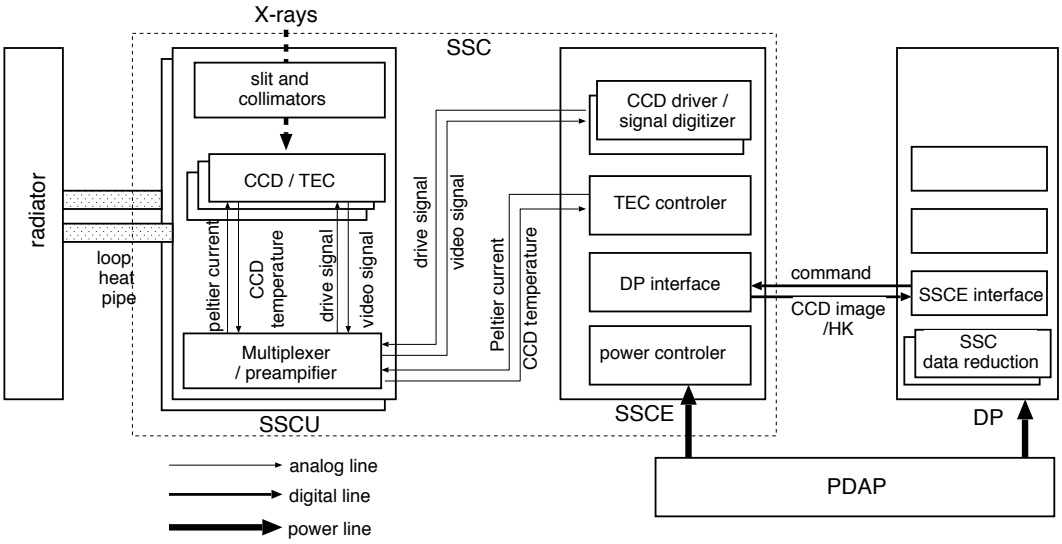

Fig. 1. Block diagram of the SSC system and signal flow between components.

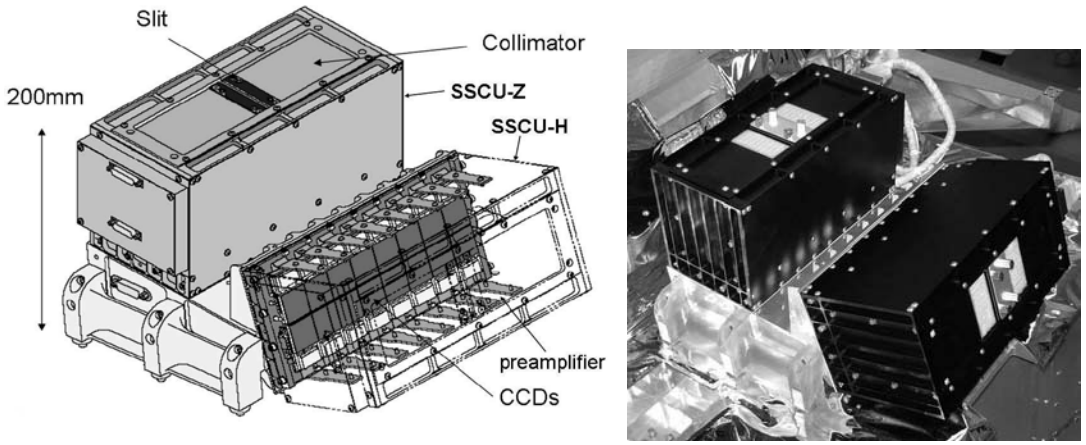

Fig. 2. Schematic view (left) and photograph (right) of SSCUs. In the photograph, protection covers are put on the slits.

The pixel number is 1024×1024, and the pixel size is 24 μm×24 μm, giving the CCD size of 25 mm × 25 mm for X-ray detection. In order to obtain the large X-ray collection area, each SSCU includes 16 CCDs, which are placed in 2×8 array as shown in Figure 2. The total X-ray detection area of 32 CCDs is $\sim$200cm^2. Charge injection (CI) is available to minimize the damage of particle radiation.

CCD has sensitivity for optical light, which degrade the sensitivity for low energy X-rays and the energy resolution. In order to block it, aluminum is coated on the CCD surface. No fragile filter is used, which makes the structure of SSCU quite simple.

SSC does not utilize X-ray mirror, hence the energy range is determined by mainly CCD. The quantum efficiency for soft X-ray is limited by the gate structure (dead layer) and aluminum on the front surface of CCD, and that of hard X-ray is by thickness of depletion layer. The gate structures is made of SiO_2 and Si whose designed thickness are 0.5 μm for both. The thickness of aluminum and depletion layer is 0.2 and 70μm, respectively. Then the energy range determined by CCD (quantum efficiency $>$ 10%) is 0.5–15keV for normally incident X-rays. The quantum efficiency for slant incident X-rays is larger for hard X-rays, and smaller for soft X-rays. Figure 4 shows the quantum efficiency of CCD as a function of X-ray energy. The detection efficiency of CCD extends to 15 keV, the energy range of SSC for hard X-ray is, however, limited by ADC. Then the energy range as X-ray camera including electronics is 0.5–12 keV.

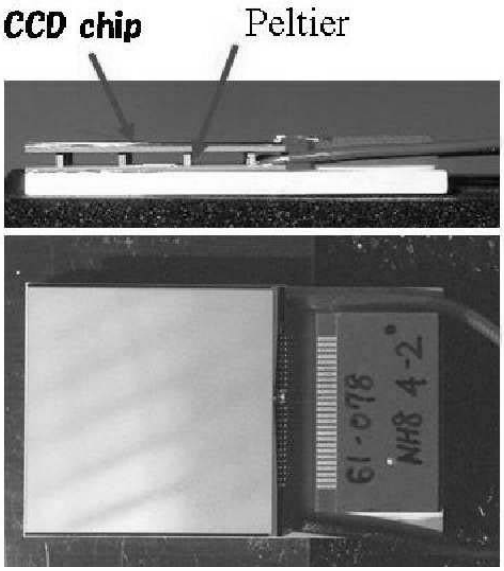

Fig. 3. A photograph of X-ray CCD equivalent to that in SSC.

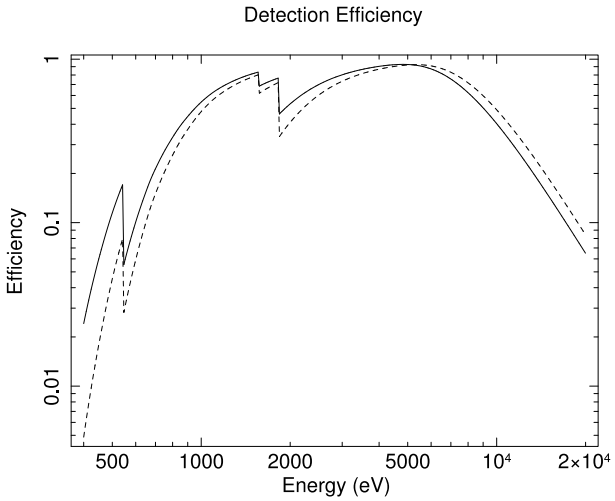

Fig. 4. The quantum efficiency of X-ray CCD as a function of incident energy calculated from the designed value of thickness of depletion layer and dead layers. The solid line represents incident angle = 0°, and the broken line is for incident angle = 40°.

2.2. Slit and Collimator

SSC has collimator and slit system but not X-ray mirrors. Collimators of SSC limit field of views (FOV) to be narrow and long shaped, and slit and CCDs determine the direction from which X-ray photons come in the narrow FOV. Figure 5 shows the design of slit and slat collimator system. This system is installed in each SSCU.

Slat collimators are made of thin sheets of phosphor bronze. The thickness is 0.1mm, and 24 sheets are placed above CCDs in the interval of 2.3 mm. The width of narrow FOV determined by slat collimators (θ_1 in Figure 5) is 1.5° in FWHM.

Slit of SSC consists of two sharp edges made of tungsten. The width between the two edges is 2.7mm. Since the position resolution of CCD is much better than the slit width, the angular resolution along the narrow FOV is determined by the slit width to be 1.5° (θ_2 in Figure 5). The angular length of the FOV (θ_3 in Figure 5) is 90°.

3. CCD Drive

CCD clocking signal is generated in SSCE. CCD is two dimension array, while SSC requires only 1-dimensional position information. Hence, multiple rows are summed in serial register at the bottom of imaging region, and the summed charges in serial register are transferred to read-out node. The number of summed rows in normal observation can be selected from 8, 16, 32 or 64 by commands. We call this number "binning" parameter. The binning of 64 is selected for the nominal observation. The larger binning gives the better timing resolution, and the better timing resolution provides better angular resolution in X-ray sky map. binning=1 is used for the diagnosis only. The clocking speed is 8μs/pixel, and a two-phase vertical transfer takes ~100 μs. The video signal from 16 CCDs in a SSCU are processed by one read-out electronics and one analog-to-digital converter (ADC). When a CCD is driven and read-out, other 15 CCDs are in exposure.

The charge injection (CI) is an effective method to restore the degraded performance of X-ray CCD (Tomida *et al.* (1997)). CI can be applied to SSC. The charge injection period is determined from the binning parameter, and the charge amount can be roughly controlled by commands through the clocking voltage. The charge-injected pixels (rows) are not summed in the serial register, and horizontally transferred without read-out. Then it takes longer time to read whole CCDs than that in non-CI operation. The operation mode with CI=ON and binning=64 reads 16 CCDs in 5.9s, which corresponds to the timing resolution in the nominal observation of SSC. The FOV of MAXI moves ~0.4° in 5.9s, which is smaller than the width of the narrow FOV (~1.5°).

Whether CI is applied or not can be controlled by command operation. CI is not required at the begining of the MAXI operation since the radiation damage would be small. However the application of CI after non-CI observation results in the significant change of the energy response. In that case, we have to construct new response functions, which is heavy and time-consuming work. Hence we decided that CI should be turned on from the beginning of the SSC operation.

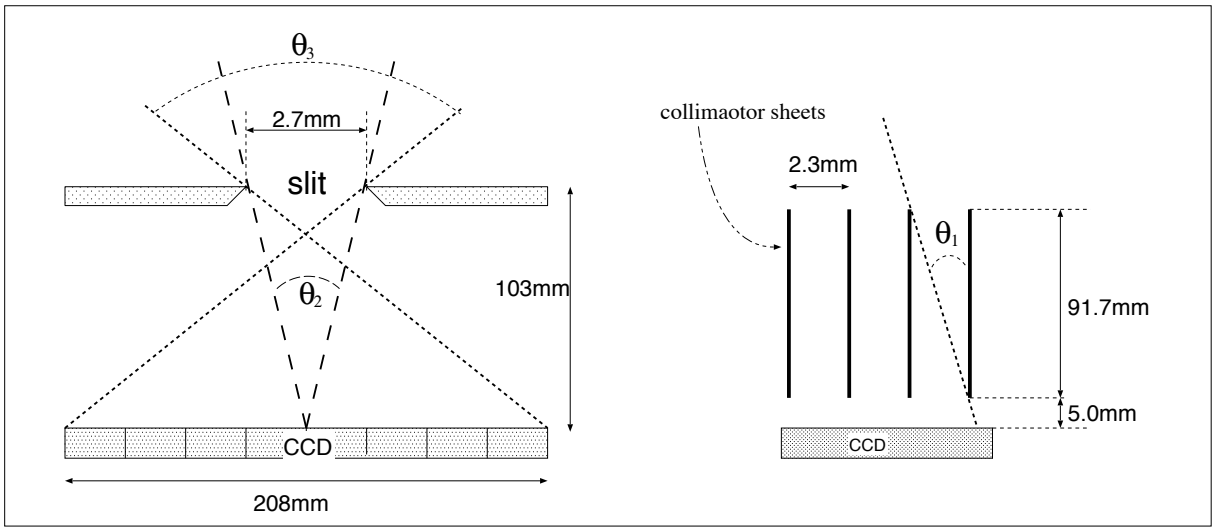

Fig. 5. Design of slit and slat collimators of SSC.

4. Data Reduction in Orbit

The CCD images digitized in SSCE are sent to DP (data processor). We designed the data reduction procedure in DP referring to that of timing mode of Suzaku/XIS (Koyama *et al.* 2007). The dark level, which is the time-averaged pixel data with no radiation of X-rays or charged particle, is determined for individual pixels and up-dated every frame.

DP searchs for the charge pattern characteristics of X-rays, which is called event. The event search is done for the pixel data after the dark-level subtraction, which we call pulse height (PH). An event is recognized when a pixel has PH between the lower and upper event threshold defined by command, and when the PH is a local maximum among adjacent 3 pixels in the row.

The MAXI telemetry data is transferred from MAXI-DP to the JEM/ISS through two physical networks in JEM/ISS. One network is MIL-1553B and another is Ethernet (Ishikawa *et al.* (this proceedings)). MIL-1553B is reliable and has much real-time connection, while the data transfer rate is limited to 50kbps at the maximum. Ethernet has data rate of 600kbps at maximum, while real-time connection is less available. It is not required that the event data in the two network should be identical. Then, we designed that Ethernet data is used for the detailed analysis (spectroscopy and diagnosis) and the MIL-1553B data is for the nova search and alert system (Negoro *et al.* (this proceedings)).

Each event data of Ethernet telemetry include CCDID, Y-address, X-address, and the PHs of adjacent 5 pixels (local maximum, trailing 2 pixels, and preceding 2 pixels). If the number of event is too large, the event data is compressed automatically or by commands. PHs of five pixels are summarized into a summed PH and the pixel pattern of the PH distribution in a row. There are 4 pixel patterns (grade 0 through grade 3), which is same as fast mode of ASCA/SIS. Grade 0 is a pixel pattern that all electrons excited by an incident X-ray is confined in one pixel.

DP compresses every X-ray event for the MIL-1553B telemetry. 14 bits are assigned for X-address and PH, and 2 bits for grade. The grade definition is same as that of Ethernet. The bit assignment for X-address and PH is determined by command. The nominal operation mode assigns 6 bits for X-address and 8 bits for PH, where 1 channel unit corresponds to 0.36 mm for position determination (X-address) and ∼60eV for energy (PH). The maximum number of SSC event for MIL-1553B telemetry is limited 254 events/16 lines.

5. Control of CCD Temperature

A one-stage thermo electric cooler (TEC) is used to cool CCDs. TEC is included in MAXI-CCD of FFTCCD-4673 (Figure 3). CCD chip is mechanically supported by TEC only, therefore heat input to the CCD is mainly thermal radiation. The heat from TEC is transferred through loop heat pipe to radiator panels on the MAXI surface, and radiated away to the space. The loop heat pipe and radiator system is designed to cool the SSCU (camera body) around -20 °C . The cooling power is determined mainly by the size of radiator ($\sim 1 m^2$). The hot side of TEC are thermally connected to the SSCU body. TEC gives the temperature difference of >40 K between CCD chip and camera body. Hence, CCD will be operated below -60 °C .

6. Pre-Flight Performance

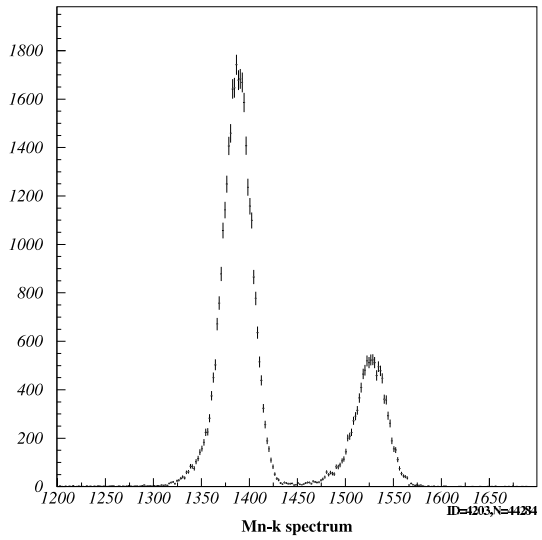

Fig. 6. Pulse height distribution of the SSC-Z/CCDID=3. X-rays from ^{55}Fe are irradiated.

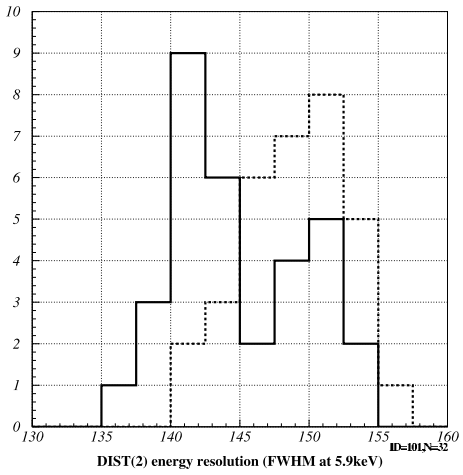

Fig. 7. The distribution of the energy resolution of 32 CCDs in SSC. The solid line is at the CCD temperature of −70°C , and the dotted line is at −60°C .

The camera level calibration of SSC was done using fluorescent X-rays from 9 materials and Mn-K X-rays from ^{55}Fe sources. The energy range is 0.52 (oxygen) to 12.5 keV (selenium).

Figure 6 shows the spectrum of ^{55}Fe sources with SSC-Z/CCDID=3. The CCD temperature is −70°C , X-rays from ^{55}Fe are irradiated, binning is 64, and the charge injection is applied (nominal operation). The spectrum is made of grades 0 events only. We can see Mn Kα and kβ lines are clearly resolved.

We fit the spectrum with two Gaussian model. One Gauusian constructs the main peak, and another Gaussian is small and resides at the lower energy side of the main peak. We defined the energy resolution as width of main Gaussian peak. The energy resolution of Figure 6 is 136 eV at 5.9 keV in FWHM, which is the best value of 32 CCDs in SSCUs. Figure 7 is the distribution of energy resolution for 32 CCDs at the CCD temperature of −60°C and −70°C . The average of energy resolution for 32 CCDs is 149eV for −60°C , and 145eV for −70°C .

The energy resolution of CCDs depends on the energy of incident X-ray. Figure 8 shows the energy resolution as a function of X-ray energy. The spectrum is made of grade 0-events only. The energy resolution is limited by mainly Fano-factor at the high energy region, and by mainly read-out noise at the low energy. The read-out noise of 32 CCDs ranges 5 to 10 electrons, which are determined from the fluctuation of PHs in horizontal over-clocked region. Charge transfer inefficiency is negligiblly small ($\sim 10^{-6}$).

Figure 9 shows the PH of SSC-Z/CCDID=3 as a function of incident X-ray energies, where PH is the channel at the center of main peak made of grade 0 events. CCD was operated in nominal parameters. We fitted the data with a linear function, and the solid line in the Figure 9 is the best fit line. We can see that the relation is well reproduced by a linear function.

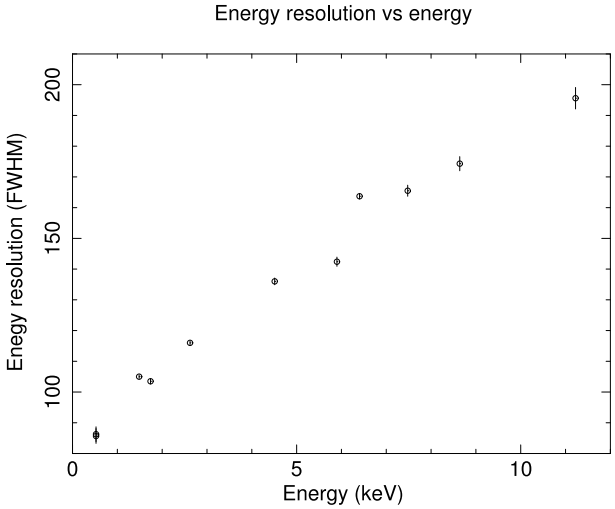

Fig. 8. The energy resolution of SSC-Z/CCDID=3 as a function of X-ray energy.

References

Burke *et al.* 1991, IEEE Trans. ED, 38, 1069
Koyama *et al.* 2007, PASJ, 59, 23
Tomida *et al.* 1997, PASJ, 49, 405
Ishikawa *et al.* This proceedings.
Mihara *et al.* This proceedings.
Negoro *et al.* This proceedings.

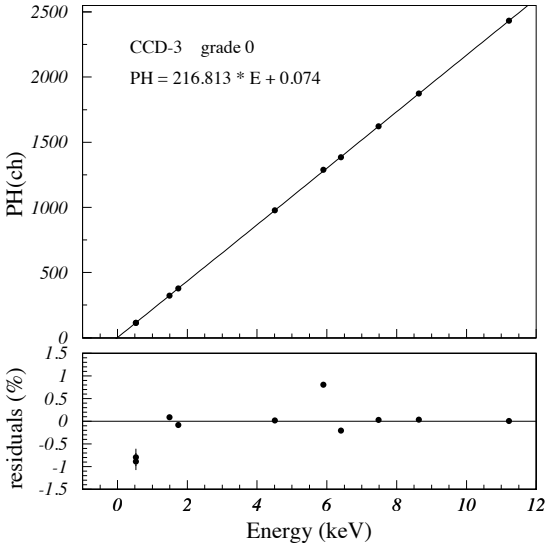

Fig. 9. Pulse height of SSC-Z/CCDID=3 as a function of X-ray energy. The lower panel shows the residuals between best fit model (linear function) and the data.